PAPER 33 (SESSION III)

Velocity of cracks extending under stress in an adverse environment

A. M. SULLIVAN
Metallurgy Division, U.S. Naval Research Laboratory, Washington, D.C., U.S.A.

Summary

The velocity of environment assisted crack propagation is reported for several titanium alloys over a range of stress intensity factor, K_I, values. Superposition of curves derived from a ligament instability model demonstrates good agreement, with the exception of some uncertainties in the threshold level, thus lending further credence to its value as a working hypothesis.

The ligament instability model of the fracture process has provided reasonable estimates of fracture toughness, K_{Ic}, through a correlation parameter, d_T, derived from comparisons of the strain for tensile instability evaluated by conventional testing. Extension of the above model to the problem of stress-corrosion enables calculation of ratio V_C (crack velocity) to V_S (an environmental parameter of surface chemical attack rate). Material flow properties, established for trials of the postulated model, are included.

Practical utilization of this approach lies in the minimal number of tests necessary to achieve usable time to fracture curves.

An interesting byproduct of this investigation, also discussed, is the effect of specimen configuration. Suitable adjustments of specimen and machine combinations can provide essentially constant fracture toughness values in a beam specimen over short segments of crack growth.

Introduction

Fracture can occur from any one of a number of causes. One of these is so-called stress-corrosion embrittlement. This nomenclature is misleading (as, unfortunately, are many other in the literature on fracture). The meaning of the term is that under stress, in a deleterious environment, cracks (or flaws) may be produced (initiation process) and will subsequently grow (propagation process) to a critical length for the load involved. At this point conditions for fracture mechanics instability are satisfied, i.e., stress intensification is equal to the fracture toughness, K_{Ic}, for the material, and rapid uncontrollable fracture occurs.

Postulates for the mechanism of this sub-critical crack growth are numerous as also are models for the instability fracture point.

Actual measurements of crack velocities over a range of fracture toughness values seemed one way of providing a few facts from which to hypothesize. Since only the propagation process is of interest here, test specimens were notched and fatigued prior to testing.

Application of ligament instability model to stress-corrosion

One simple and attractive descriptive model of the fracture process assumes that a discrete ligament ahead of the crack attains tensile instability

strain and separates, transferring the strain intensification to the next ligaments in a progressive sequential manner [1, 2]. This hypothesis derived from concentrated and serious efforts to relate the fracture toughness parameter K_{Ic} to material plastic flow properties. The impetus for this research was the fact that fracture toughness values can be very difficult to measure. Necessitating an elastic condition at the crack tip, test specimen size cannot be standardized. For materials of high toughness and low yield strength, the size requirement can exceed the capacity of conventional test equipment. Obviously, a correlation parameter which would permit estmates of fracture toughness from conventional material property tests would be practical.

Initial indications [3] that comparison of K_{Ic} and yield strength (σ_{YS}) would satisfactorily resolve this problem proved fortuitous. When strain was considered the relevant property, however, a satisfactory correlation was established containing the instability strain, then considered equal to the strain hardening exponent, n [4].

$$K_{Ic} = E\sqrt{2\pi d_T n} \tag{1}$$

Here d_T, a distance from the crack tip called the process zone, was found to be constant and was considered as the ligament subjected to tensile instability. That its size may be defined by some microstructural feature has been demonstrated for steels of varied sulfur content [5].

An application of this model to stress corrosion (propagation) requires definition of tensile instability in terms of area – such that strain hardening, $d\sigma/d\epsilon = \theta$, has diminished with increasing strain where it is just sufficient to counteract the diminution of load carrying capacity due to areal contraction.

$$A\left(\frac{\partial\bar{\sigma}}{\partial\bar{\epsilon}}\right)\left(\frac{d\epsilon}{dt}\right) = \bar{\sigma}\left(\frac{dA}{dt}\right) \tag{2}$$

Without reproducing all of the argument, it suffices to say that area is diminished by the normal Poisson contraction behavior and may be diminished by some process dependent upon environment which provisionally has been termed the surface attack rate, V_S. Now equation 2 becomes

$$A\left(\frac{\partial\bar{\sigma}}{\partial\bar{\epsilon}}\right)\left(\frac{d\epsilon}{dt}\right) = \bar{\sigma}\left(2\nu A\frac{d\epsilon}{dt} + \pi d_T V_S\right) \tag{3a}$$

$$\left(\frac{\bar{\theta}}{\bar{\sigma}} - 2\nu\right) = \frac{4V_S}{d_T\,\dot{\epsilon}} \tag{3b}$$

where $\bar{\theta} = d\bar{\sigma}/d\bar{\epsilon}$.

Substitution of a crack velocity for $\dot{\epsilon}$ (differentiation of equation 1) provides the equivalency

$$\frac{V_S}{V_C} = \frac{\epsilon}{8}\left(\frac{\bar{\theta}}{\bar{\sigma}} - 2\nu\right) \tag{4}$$

The right side of this equation can be readily evaluated from details of the stress-strain curve.

With this relationship in mind, actual crack velocity data proved most instructive.

Materials

Two titanium alloys were chosen for investigation; these exhibited somewhat different stress-corrosive properties [6].

A	90Ti	7Al	2Cb	1Ta
B	90Ti	8Al	1Mo	1V
	A		B	
σ_{YS} Ksi	110·6		112·0	
K_{Ic} Ksi$\sqrt{\text{in}}$	85·0		120·0	
K_{Iscc} Ksi$\sqrt{\text{in}}$	24·0		45·0	
ϵ_c %	16·2		8·13	
$d_T \times 10^{-6}$ in	151		1198	

Specimen configuration

The various specimen types utilized are discussed below.

1. *Notched beams – NB*

Beams were 7 in long with a 6½ in span ($2L$) and 1$^{7}/_{16}$ in depth (W) of varied breadth (B) = 1 to 1½ in. For initial experimentation these were not side notched. The crack path is somewhat irregular, however, and several tests with side notched beams have been run.

The initial crack length, a_0, was such that a_0/W approximated 0·30; this includes a fatigue crack at the end of the slotted notch machined with a 60° angle of about 0·01" radius (Charpy cutter) at the tip.

The three point bending roller bearing jig found necessary to avoid excessive hysteresis upon unloading is seen in Fig. 1.

2. *Single edge notch – SEN (side notched)*

Rather large SEN specimens were employed (2 in wide (W) by 6 ins long (L)) between pin holes for loading. A tendency was noted for the crack path to lie outside the side-groove root. In addition, due to testing machine capacity, the thickness requirement (B) could not be met for materials of the fracture toughness (K_{Ic}) and yield stress (σ_{YS}) being investigated. Again, a_0 was such that $a_0/W \cong 0{\cdot}3$.

3. *Compression cylinders*
Compression specimens ¼ in diameter with a 7/16 in length were used. The cylindrical axis was chosen perpendicular to the crack plane of the fracture specimen.

Experimental procedures and data reduction
To be of practical value, a section described by the above title should contain exhaustive details of the operations involved. It is hoped that the (necessarily) abridged version provided here will be helpful.

1. *Crack length measurement calibrations*
Compliance, the slope of the deflection – load curve, δ/P, of any specimen configuration containing a crack varies with crack length, so also does the slope of the crack-opening displacement – load curve, COD/P. Therefore, a specimen of geometry identical to that of the test specimen is used for calibration. A series of load-cracking opening displacement curves, are run (three at least for each crack length) as the notch is progressively deepened.

A suitably normalized curve is then plotted, $EB\delta/P$ versus a/W. When the test is run, straight lines are drawn from the origin to selected load points, Fig. 2. When these slopes are appropriately normalized (multiply by EB) the value of a/W can be read from the calibration curve and thus crack length, a, obtained for known loads.

2. *Fracture toughness calculations*
For both notched beams and single edge notched specimens the functional relationships between K, load, and crack length are those proposed by Brown and Srawley [7].

3. *Determination of material flow properties*
In this laboratory, it has been found convenient to utilize compression specimens for determination of material flow properties. A four-lobed gage is calibrated to give strain measurement in terms of areal strain ϵ_A. A typical curve is shown in Fig. 3. Significant relationships for evaluating V_S/V_C according to equation 4 are:

$\epsilon_A = \epsilon_A$ plastic $+ \sigma_e/\theta_0$
$\bar{\theta} = \theta - \sigma_e$
$\bar{\sigma} = \sigma/1 + \epsilon_A$

Further amplifying equation 1 where these are longitudinal strains,

$$K = K_{Ic}\left(\frac{\epsilon_L}{\epsilon_e}\right) \qquad (5)$$

$\epsilon_L = \epsilon_A$ (plastic) $+ \sigma/E$, ϵ_e, the strain hardening exponent or critical strain at instability, is the value of strain at the point where $\bar{\theta}/\bar{\sigma} = 1$ and may be determined as in Fig. 4.

Plots of K_I so determined against V_S/V_C are shown in Fig. 5.

Testing machine and instrumentation
Tests were made using the Krafft-Hahn DUL machine developed at NRL. This can be operated at either constant load or constant head displacement

Fortuitously, it developed that, at constant head displacement, the machine stiffness was such that for relatively short increments of crack extension the unloading curve parallelled the constant K envelope; under this condition cracks extended at constant velocity.

The output from a four point Bridge (SR-4 strain gages) affixed to the various weigh bars coupled to the loading piston is calibrated to read load, P.

Crack opening displacement, COD, is measured by a joined pair of cantilever beams, Fig. 1, spring fitted into a seat provided on the specimen. Here the SR-4 bridge output is calibrated to read in ins.

Bridge outputs for P and COD are simultaneously recorded on a Moseley X-Y instrument. Information developed in this manner provides crack length, a, which coupled with load, P, measurement, can be used to determine stress intensity, K, values.

Time can be recorded in several ways:

a. For very slow growth, 60, 30, or 15 min intervals are manually indicated on the chart.

b. When the rate of crack growth is somewhat faster, an amplification of the horizontal signal is effected by using the min hand of a Gra-Lab Universal Timer to close a microswitch circuit to a dry cell battery.

c. For still more rapid crack growth, signal amplification is provided by the output of a time-mark generator (Tektronix Type 184), appropriate intervals being selected.

This timing system is obviously not automatic, requiring the presence of an attendant whose judgement is reliable.

Testing conditions
All specimens were cleaned prior to testing in an ultrasonic cleaning bath with fresh acetone.

A polyethylene laboratory bottle or beaker (chosen for size) was cut down to fit over the specimen. This serves as a container for the environmental medium, Fig. 1, and may be affixed to the specimen using Fisher's 'Pyseal' cement, an inert low melting point compound. However, this is rather brittle and cannot accommodate much specimen deformation. An uncured rubber adhesive, General Electric Company 'RTV-102' is more flexible, but must be cured before using bath (8-10 hrs in air).

After positioning the specimen in the machine, solution is introduced into the bath with a hypodermic syringe or flexible wash bottle taking care that the fluid level covers the crack tip but is not high enough to impinge on the gage used for COD detection and thus introduce unwanted galvanic action.

The environment used was a 3·5% sodium chloride distilled water solution. For time to fracture tests, it has been established that this medium gives values identical to those found using naturally occurring sea water [8].– despite the greater chemical complexity of the latter.

Discussion of experimental results

A nice discrimination between the two titanium alloys is readily apparent, Fig. 6. Further, superposition of the V_C/V_S curve from Krafft's ligamental model analysis is seen to correspond well with the data presented when K is below K_{Ie}. Superposition of the two plots K_I vs. log V_C and K_I vs. log V_C/V_S and translation across the log axis will give $V_C/V_C/V_S$ and thus determine the value of V_S. Returning to equation 4, if V_S is assumed constant, a failure time integral can be expressed as

$$V_S \frac{K_{Ie}}{K_0} \frac{1}{V_C} \Delta a = V_S t_f$$

Knowing the K_I level at a_0, the increase relative to it at any absolute extension, Δa, will be constant. Having computed these percentages, numerical integration will provide a K_I vs. time to failure plot for comparison with a customary form of stress-corrosion data.

In Fig. 7 this comparison is shown and the observed data points lie near the calculated curves.

Values of K greater than K_{Ie} in general correspond to situations where β (= $(K/\sigma_{YS})^2 1/B$ or β^1 (= $(K/\sigma_{YS})^2 1/W-a$ exceed reasonable figures for plane strain conditions (min 0·5, max 1·0). Below K = 80 Ksi in, there appear to be two K vs. V_C curves for the 7-2-1 alloy. Three of the four upper curve SEN tests were loaded and unloaded prior to data taking, but this is not true of the NB test upper curve. All SEN points are above $\beta > 0{\cdot}50$ but again not true for NB test. The lower curve SEN data points are from two specimens with different types of side groove notches; one a 60°, root radius ca. 0·10; the other a curve groove radius 1/8. Thus, no immediate explanation can be offered for this apparent inconsistency.

The fractured surfaces, however, are very rough; so it may be that branching and proliferation of the advancing fracture causes erroneous estimates of crack length which is reflected in both K and V_C values. The obvious fact of considerable spread in the data scatter favor the explanation.

Some data also indicate that the blunting associated with the crack's advance in salt water is raising the apparent K_{Ie} value. The standard practice of extending a machined notch by fatigue to provide a sharp 'natural'

crack arose from observations that larger crack roof radii gave higher K_{Ic} values. If this is true, using the higher value for matching would tend to raise K_0 and improve the correlation. Extension of the research to elucidate this point is in progress.

The data unfortunately re-emphasize the troublesome point that at low fracture toughness stress intensity values, cracks will grow in the presence of a deleterious environment and quite rapidly – (one inch in 2·8 hrs at K – 30 and 0·55 hrs at K – 40 for the better titanium 7-2-1).

For definition of the threshold stress, K_{Iscc}, below which cracks do not propagate, it is considered [2] that a triaxiality factor

$$T.F. = \frac{1}{1-2\nu} \tag{6}$$

will operate to augment the elastic strain, thus

$$\epsilon_0 = T.F. \frac{\sigma_0}{E} \qquad \sigma_0 = \text{Proportional limit}$$

and

$$K_0 = K_{Ic} \frac{\epsilon_0}{\epsilon_c} \tag{7}$$

For titanium alloys, it is found that the threshold value is generally underestimated by this analytic method which defines it well for both aluminum alloys and brass [2]. It has been suggested that anisotropy, very prevalent in titanium alloys, is responsible for this effect. Further clarification of this important point is mandatory.

Conclusions

1. The velocity of environment induced crack propagation as a function of fracture toughness K_I indicates substantial agreement with the ligament instability model for crack extension which postulates a constant value of V_S.
2. Further clarification is necessary to define the threshold value of K_0 assumed equivalent to K_{Iscc}.
3. The apparent smooth curve of K vs. V_C at values in excess of K_{Ic} is anomalous and requires explanation.

Acknowledgments

It is a pleasure to acknowledge the stimulation afforded by the provocative model of the author's colleague J. M. Krafft. The expert and untiring assistance of F. W. Bird made the experimental work possible. The initial impetus arose from support by the Advanced Research Projects Agency as part of the ARPA Coupling Program on Stress Corrosion Cracking and was carried on in the Metallurgy Division, W. S. Pellini, Superintendent.

References

1. KRAFFT, J. M. 'Role of local dissolution in corrosion-assisted cracking of titanium alloys', Report of NRL Progress, p. 6, March, 1967.
2. KRAFFT, J. M. & MULHERIN, J. H. 'Tensile-ligament stability and the slow growth of cracks in alloys of iron, aluminum, copper and titanium, forthcoming publication.
3. KRAFFT, J. M. & SULLIVAN, A. M. 'Effect of speed and temperature on crack toughness and yield strength in mild steel', *Am. Soc. Metals, Trans. 56:* p. 160, March, 1963.
4. KRAFFT, J. M. 'Correlation of plane strain crack toughness with strain hardening characteristics of a low, a medium, and a high strength steel', *Appl. Mat. Res.*, vol. 3, p. 88, April, 1964; 'Fracture toughness of metals', Report of NRL Progress, p. 4, November, 1963.
5. BIRKLE, A. J., WEI, R. P. & PELLISSIER, G. E. 'Analysis of plane strain fracture in a series of 0·45C, Ni-Cr-Mo steels with different sulfur contents', *Am. Soc. Metals Trans.*, vol. 59, p. 981, 1966.
6. JUDY, R. W. Jr. & GOODE, R. J. 'Stress-corrosion cracking characteristics of alloys of titanium in salt water', Naval Research Laboratory Report No. 6564, July, 1967.
7. BROWN, W. F. Jr. & SRAWLEY, J. E. 'Plane strain crack toughness testing of high strength metallic materials', *ASTM Special Technical Publication No. 410*, p. 9ff, 1966.
8. BROWN, B. F., FORGESON, B. W., LENNOX, T. J. Jr., LUPTON, T. C., NEMBEGIN, R. L., PETERSON, M. H., SMITH, J. A. & WALDRON, L. J. 'Marine corrosion studies', Naval Research Laboratory Memorandum Report No. 1634, July 1965.

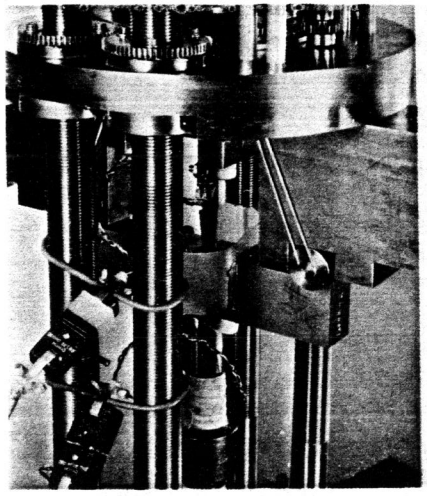

Fig. 1. Notched beam positioned in three point loading roller bearing jig in loading frame of DUL testing machine. The polyethylene environmental bath surrounds the notched region and the COD detection beams are located in the notch.

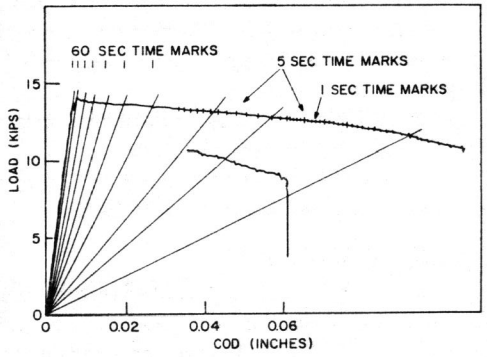

Fig. 2. Typical load-crack opening displacement curve for Ti alloy 7-2-1 indicating COD/P slopes for crack length determination and showing time marks.

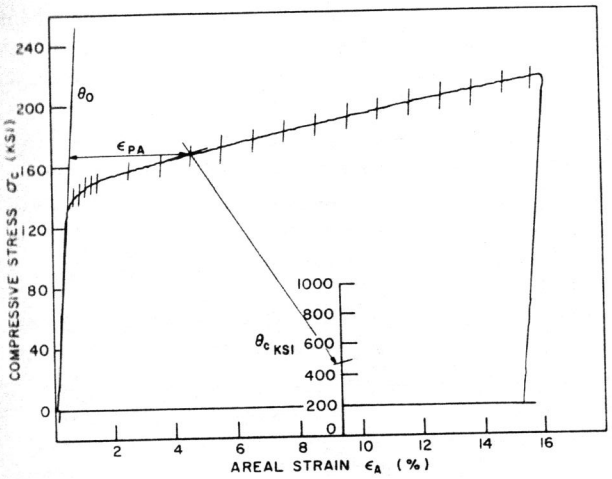

Fig. 3. Typical stress-strain (σ vs. ϵ_A) curve for a compression cylinder of Ti alloy 8-1-1. Vertical marks indicate strain stations for stress (σ) and strain hardening rate ($\theta = d\sigma/d\epsilon$) determination.

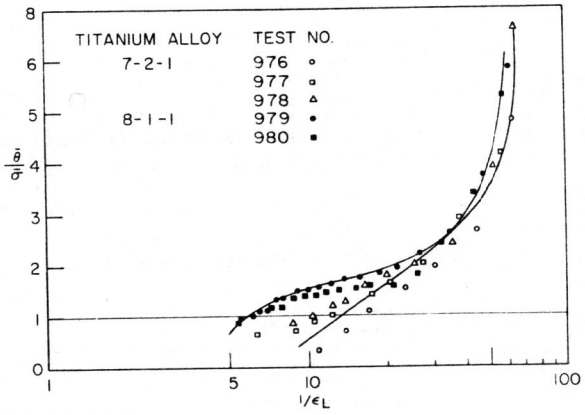

Fig. 4. $\bar{\theta}/\bar{\sigma}$ versus log $1/\epsilon_L$ evaluates critical instability strain (ϵ_c) at $\bar{\theta}/\bar{\sigma} = 1$. Data spread is not dissimilar to that of fracture toughness data.

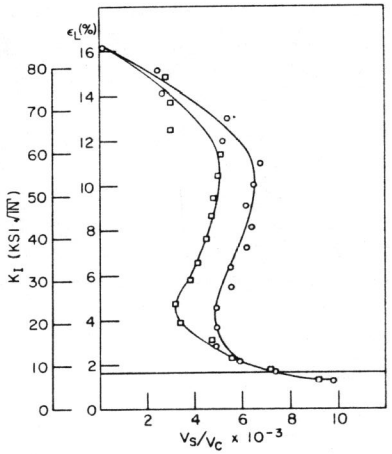

Fig. 5. K_I proportional to ϵ_L (eq. 5) plotted against V_S/V_C again shows typical data scatter for two tests of Ti alloy 8-1-1.

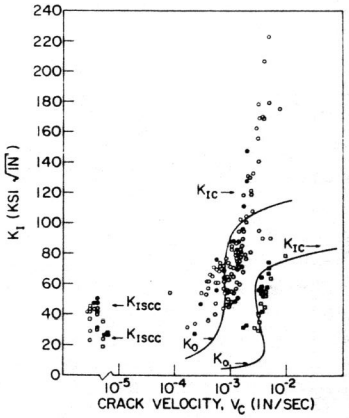

Fig. 6. Stress intensity, K_I is plotted against crack velocity, K_I, K_{I_c} $K_{I_{sec}}$ and K_0 are indicated for the two titanium alloys tested: Ti 7-2-1 ○; Ti 8-1-1□. Open symbols are from tests run at constant load; closed are those run at constant head displacement. Note data scatter similar to that seen in compression curve data analysis.

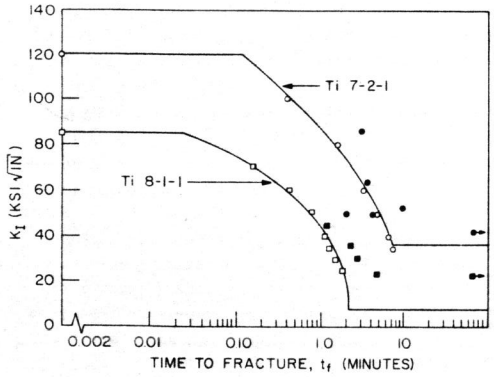

Fig. 7. Stress intensity, K_I, is plotted against time to fracture; curves are drawn through (open) points computed from equations of the ligament instability model while time-to-fracture data (solid) points are plotted.